



# Theoretical performance on energy and exergy analysis of methyl esters of rubber seed oil fuelled on supercharged VCR engine

S. Murugapoopathi<sup>1</sup> · T. Ramachandran<sup>2</sup> · C. Rajaganapathy<sup>3</sup>

Received: 6 April 2021 / Accepted: 16 August 2022  
© The Author(s), under exclusive licence to Springer Nature B.V. 2022

## Abstract

Bio-fuels derived from sustainable resources provide reliable energy for future needs in a wide range of industries. In this work, biodiesel made using renewable rubber seed oil is transesterified and suitably mixed with diesel at 20%, 40%, 60% and 80% in single-cylinder four-stroke direct injection, variable compression ratio engine. Experiments are conducted by changing supercharging as 1 atm., 1.25 and 1.5 bar pressure measured at inlet air pipe with an average compression ratio of 20 at fixed speed of 1500 rpm at 80% load for various fuel blends. The effect of supercharging reduces the cooling water loss by 4.11%, and unaccounted losses slightly increase by 2.64% for averaged fuel blends and compression ratio. The shaft energy improves by 4.31%, and exhaust gas energy flow decreases by 5.18% for the same operating conditions. The improved BTE by 2.99% with reduction in BSEC of 7.54% are witnessed with supercharging. Peak pressure rises by 3.75% with supercharging but slight drop in heat release rate observed by 4.46% for same operating conditions. The entropy generation and exhaust gas availability decrease by 18.56% and 4.86% with supercharging. The destructed irreversibility and cooling water availability were declined by 11.97% and 22.51% with supercharging. The exhaust emissions of CO and HC emissions were found to be decreased by 10.26% and 21.41% with supercharging compared with diesel. The second law efficiency was improved by 9.51% with supercharging for averaged fuel blends and compression ratio.

**Keywords** Energy analysis · Exergy analysis · Biodiesel · Supercharging · Availability

## Abbreviations

CR      Compression ratio  
SC      Supercharging

---

✉ S. Murugapoopathi  
poopathism@gmail.com

<sup>1</sup> Department of Mechanical Engineering, PSNA College of Engineering and Technology, Dindigul 624622, India

<sup>2</sup> Faculty of Engineering and Technology, Department of Automobile Engineering, Jain (Deemed-to-Be University), Bengaluru 562112, India

<sup>3</sup> Department of Mechanical Engineering, Government College of Engineering Srirangam, Trichy, Tamilnadu 620012, India

RSO	Rubber seed oil
HC	Hydrocarbon emission (ppm)
VCR	Variable compression ratio
HRR	Heat release rate ( $J/^\circ CA$ )
CO	Carbon monoxide emission (%)
BTE	Brake thermal efficiency (%)
BSEC	Brake specific energy consumption (kJ/s/kW)
$NO_x$	Nitrogen oxides emission (ppm)
SC	Supercharging
B20	Biodiesel (20%) + Diesel (80%)
B40	Biodiesel (40%) + Diesel (60%)
$CO_2$	Carbon dioxide emission (%)
NAE	Naturally aspirated engine
EGT	Exhaust gas temperature ( $^\circ C$ )
LHV	Lower heating value of fuel (kJ/kg)
SCE	Supercharged engine
FFA	Free fatty acid
SFC	Specific fuel consumption (kJ/kg/K)
IP	Injection Pressure (bar)
CA	Crank angle

### List of symbols

$g$	Gauge pressure (bar)
$P_{max}$	Maximum pressure (bar)
$S$	Entropy generation (kJ/K)
$A_d$	Destructed availability
$A_{in}$	Fuel input availability
$\eta_{II}$	Second law efficiency (%)
$R_u$	Universal gas constant (kJ/kg/K)
$A_s$	Shaft availability
$E_{ci}$	Exhaust gas calorimeter water inlet
$T$	Temperature
$C_{pe}$	Specific heat of exhaust gas (kJ/kg/K)
$A_w$	Cooling water availability
$P_e$	Pressure of exhaust gases (bar)
Amb	Ambient
$A_e$	Exhaust gas availability
$Q_{in}$	Heat input (kW)
$C_{pw}$	Specific heat of cooling water (kJ/kg/K)
$E_{wi}$	Engine cooling water inlet
$Q_s$	Brake power (kW)
$M_a$	Mass of air (kg/s)
$M_f$	Mass of fuel (kg/s)
$Q_w$	Heat lost by cooling water (kW)
$E_{wo}$	Engine cooling water outlet
$A_u$	Uncounted availability
$Q_u$	Unaccounted heat loss (kW)
$E_{co}$	Exhaust gas calorimeter water outlet

$N$	Speed (rpm)
$Q_{in}$	Heat input (kW)
$W$	Load (kg)
$R$	Radius of brake drum (m)

## 1 Introduction

Alternate fuels play a dominant role in world energy scenarios, especially in diesel engines. Most of the research was performed to find a way to replace fossil fuel due to its scarcity and depletion in upcoming years. Nowadays, many alternate energy resources are being introduced in different fields like transportation, industry, agricultural fields, aeronautics, commercial and public sectors, subsequently. However, diesel engines are used in many industrial, power, energy, and agricultural sectors for their reliability and wide range of operation. It has the advantages of improved torque, better power to weight ratio, supercharging, good performance, less fuel consumption, and low maintenance (Giakoumis & Rakopoulos 2006). The energy and exergy of a single-cylinder VCR engine powered by water emulsified palm oil methyl ester (POME) were examined. The CR for biodiesel was 17, 17.5, and 18 degrees Celsius, whereas the IT was 20, 23, and 28 degrees Celsius. At higher CR of 18 and 20° before top dead center (BTDC) in the 3.5 kW diesel engine, achievable shaft energy increased. At these operational conditions, over 40% of fuel energy was absorbed from the fuel (Debnath et al., 2013). An energy and exergy analysis was carried out on a low-displacement diesel engine running on diesel, POME10 with and without hydroxy gas at different flow rates of 0.075, 0.15, and 0.255 LPM at a constant speed under 20 to 100% loading. The peak pressure and heat release rate were intensified with hydroxy gas at 11.86% and 15.85%, respectively. HC and smoke emissions were reduced by up to 11.02% and 9.39% with hydroxy gas in comparison with POME10 (Duarte-Forero et al., 2021). A low-temperature, closed-cycle diesel engine with diesel and methane dual-fuel was simulated to improve the fuel efficiency of the engine. Exergy transformation was analyzed by varying crank angle degrees (CAD) from 300 to 340 at 6 bar brake mean effective pressure. At CAD 310, the fuel conversion efficiency was increased to 43.6% and the second-law efficiency to 52.2% (Mahabadipour et al. 2019). Thermodynamic analysis was carried out using oxygenated fuel-based diesel, waste cooking biodiesel, and triacetin. Lower exhaust energy loss was observed with improved thermal efficiency using oxygenated fuel. The thermal efficiency of B100 was 5% greater than diesel, with the least amount of energy lost in the exhaust. The second law efficiency is improved by 10% with oxygenated fuel, and the destructive availability is reduced by 29% with triacetin added to B100 (Odibi et al., 2019). Diesel, hazelnut biodiesel, and canola biodiesel were tested for energy and exergy at different operating speeds of 1500, 1800, 2100, and 2400 rpm. Thermal efficiency and exergy efficiency were observed to be at their peak at 1800 rpm. For all tested fuels, the losses due to destruction were 45.45%, 47.36%, and 47.41%, respectively, compared to other operating speeds. (Şanlı & Uludamar, 2020). Taguchis' design matrix was used to identify the optimum energy and exergetic performance of a diesel engine using waste cooking biodiesel under three operating levels such as speed (1300, 1600, 1900, and 2100 rpm), load (25, 50, 75, and 100%), and blend (0, 20, 40, and 60%). The highest BTE has been observed for B20 at level 1 and the highest exergy efficiency for B0 at level 2. B0 and B20 give the lowest exergy destruction compared to other blends. CO and CO<sub>2</sub> emissions decreased as the

biodiesel blend in diesel increased (Chaudhary & Gakkhar, 2021). Biodiesel and butanol were investigated to improve the CI engine's energy and energetic performance. The diesel engine's highest energy-exergy efficiency improvements and sustainability index (SI) were 32.49%, 30.25%, and 1.434%, respectively, when utilizing B100 fuel at 1400 rpm. According to the performance of the energy-exergy and SI, D75B20But5 can be considered as the fuel with the best fuel ratio (Sarıkoç et al., 2020). The cottonseed biodiesel of 5,10, and 15% blended with diesel was tested in a 3.5 kW, 3500 rpm diesel engine to improve the engine output power, energy, and exergy efficiency. The exhaust loss was decreased by 20% for B15 than for conventional diesel, but 8.46% power loss occurs at an optimum engine speed of 2500 rpm (Gnanamani et al., 2021). Rubber seed oil methyl ester (ROME) was tested in a single-cylinder VCR engine with different CRs and blends at 80%. When CR is increased, exergy efficiency improves by 4.19 percent, and entropy generation falls by 18.27 percent when compared to diesel. The CO and HC emissions decrease by 3.63% and 33.08%, respectively, upon an increase in CR compared to diesel (Murugapoopathi & Vasudevan 2019b).

The research reviewed above focused on energy and exergy analyses, with just a few investigations on bio-fuel combinations in the CI engine employing load, blend and CR modifications. It was known exactly compression ratio and supercharging work together in a VCR engine running on biodiesel mixtures. This study attempts to determine the best engine operating conditions in a VCR engine by altering the compression ratio from 18:1, 19:1, 20:1, 21:1, and 22:1 and changing the supercharging pressure from 1.25 to 1.5 bar at 80 percent load and 1500 rpm. The studies were carried out on diesel, B20, B40, B60, and B80 for the author's optimal blends (Murugapoopathi & Vasudevan 2019a). Using the above-optimal compositions in a VCR engine, the energy and exergy of fuel inflow, brake power, cooling water, and exergy destruction are addressed. Meanwhile, studies have been directed at the effects of CR and supercharging on peak pressure, heat release rate, BTE, the mass of fuel inducted, exergy efficiency, and entropy generation.

## 2 Experimental investigation of Test set up

Rubber seed oil that had been collected around was used to make biofuel in this experiment. Because of free fatty acid (FFA) level (Table 1) of RSO oil was greater than 2%, a two-step transesterification procedure was used to make biodiesel. One liter of hot oil was added to 300 mL of solvent in the first step. The oil was then combined with 4 mg of sulfuric acid to eliminate the acid present in the oil. To extract bio-fuel from RSO,

**Table 1** Free fatty acid composition of rubber seed oil

Fatty acid	Structure	Formula	Composition (wt. %) <sup>d</sup>
Palmitic acid	C16:0	$C_{16}H_{32}O_2$	10.2%
Stearic acid	C18:0	$C_{18}H_{36}O_2$	8.7%
Oleic acid	C18:1	$C_{18}H_{34}O_2$	24.6%
Linoleic acid	C18:2	$C_{18}H_{32}O_2$	39.6%
Linoleic acid	C18:3	$C_{18}H_{30}O_2$	16.3%

the oil (1 L) was heated and combined with methanol (300 mL) in the presence of KOH (4 g) as a reagent in the second step. When rubber seed oil was extracted from glycerin and heated to around 80 °C to remove water particles, the methyl esters were produced. For fuel preparation, biodiesel was blended with diesel at a ratio of 20% to 40%. RSO biodiesel was tested in a research center and found to fulfill ASTM diesel standards (Table 2).

The test engine was a VCR (Kirloskar) water-cooled direct injection engine. Table 3 specifies the engine test conditions. The compression ratio was altered from 18:1 to 22:1 with a one-percentage-point increase by moving the spindle provided in the engine head assembly. For each revolution, the crank angle encoder detects motion. The exhaust gas calorimeter has an outlet pipe that may be used to measure temperature at different locations using K (Aluminum) type thermocouples. An air tank, manometer, air blower, and pipette were included in the experimental setup. The combustion pressure was measured via the Kistler transducer type sensor. The fuel flow was measured by the electronic solenoid control switch. Rota meters direct the flow of cooling water to various areas of the engine and calorimeter. An eddy current dynamometer with a load cell was connected to the engine crankshaft. A data acquisition system connects several sensing units, which was then sent to a personal computer for further processing.

The investigational layout of the VCR engine system is shown in Fig. 1. In a naturally aspirated condition, an engine was powered through a diesel at CR 18:1 at 1500 rpm. To achieve a stable load, an engine was gradually loaded (80% load). To maintain steady-state temperatures, the Rota meter flow rate was kept at 60 mL/sec. On a personal computer, the experimental values of fuel flow, inlet air pressure, temperatures, airflow, engine speed, and in-cylinder pressure were sensed and recorded. The test was performed with different CRs (19:1, 20:1, 21:1, and 22:1) and supercharging (1.25 bar and 1.5 bar). The trials were repeated three times, with the average data used in the calculations. The uncertainty in measurements and its resolution of emission parameters are provided in Table 4 and Table 5.

**Table 2** Properties and Indian standards of biodiesel and diesel

Properties	Diesel	B20	B40	B60	B80	B100	Biodiesel standards <sup>a,b</sup>	
							ASTM D 6751–02	IS 1448/ DIN EN 14,214
Density (Kg <sup>m</sup> <sup>-3</sup> )	0.835	0.82	0.86	0.87	0.88	0.89	–	0.86–0.90
Viscosity at 40 °C(mm <sup>2</sup> s <sup>-1</sup> )	1.382	1.143	1.232	1.45	2.24	3.42	1.9–6.0	3.5–5.0
Flash Point	42 °C	50 °C	56 °C	65 °C	120 °C	210 °C	> 130	> 120
Fire Point	65 °C	54 °C	60 °C	75 °C	160 °C	230 °C	–	–
Calculated cetane index	45–55 <sup>c</sup>	49	47	45	41	39	41 min	51 min
Gross calorific value (KJ Kg <sup>-1</sup> )	45200 <sup>c</sup>	41,343	40,200	39,129	38,070	36,986	–	–

Reference Mahabadipour et al., (2019)

Reference Murugapopathi and Vasudevan, (2019a)

Reference Murugapopathi and Vasudevan, (2019b)

**Table 3** Specification of the variable compression ratio engine

General details	Make and specifications
Engine	Variable compression ratio, direct injection, water cooled engine
Make	Kirloskar make—single cylinder
Engine capacity	736 cc
Oil capacity	3.2 L
Power	5 HP at 1500 rpm
Loading system	Eddy current dynamometer
Power transmission	Through load cell
Type	Stain gauge based load cell
Range	0–50kgs
Make	Techno-make
Maximum torque	95 N-m at 1500 rpm
Speed measurement	Digital tachometer and proximity sensor
Make	MECO
Sensor	Non-contact type PNP sensor
Range	0–9999 rpm
Loading and unloading	Solid state microprocessor controller
Pressure sensor	Kistler make
Range	0–250 bar
Type	Piezoelectric – air cooled
Fuel injector	Bosch Make
Crank angle encoder	Kubler make
Pulse count	360 PPR
Connector	type 9416, 12-pin, type 9416L, 12-pin
Air tank	500 mm cubic mild steel
Air measurement	DP sensor with inline transmitter
Range	100 mm
Fuel tank	7.5 L mild steel
Fuel measurement	Optical liquid level sensor constant volume, fully automatic and burette
Range	0- 50 cc
Temperature measurement	“k” type (Alumel-chromel) 0–1200°C
Water flow	Rota meter – Acrylic
Range	40–400 LPH (Engine cooling)
Exhaust gas calorimeter type	Shell and tube—stainless steel
Cross section	Square ( 400 mm × 400 mm)
Range	10-100LPH (Calorimeter cooling)
Data acquisition system	32 bit micro controller
Data frequency	250 Ks/S
Operating voltage	3.3 V
Software	Engine test express for engine combustion analysis and performance software
Gas analyzer	Mars Tech – MN -05 model
NOx sensor	Envitech – Germany make
Oxygen sensor	Citytech – UK make
HC, CO sensor	NDIR type

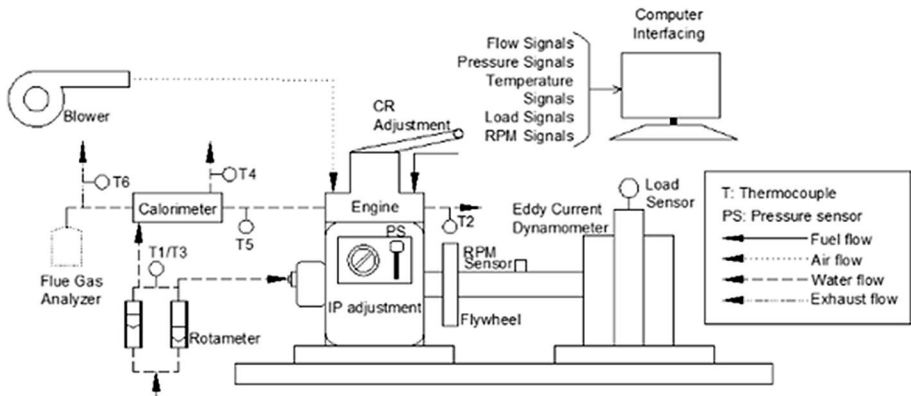


Fig. 1 Schematic lay out of VCR engine set-up

Table 4 Uncertainty in measurement

Measurements	Accuracy
Engine speed	± 11 rpm
Time	± 0.20%
Specific fuel consumption	± 1%
Temperature	± 2 °C
Crank angle encoder	± 0.5°CA
Piezoelectric sensor	± 0.50%
Carbon monoxide	0.02%
Hydrocarbon	0.05%
Carbon dioxide	0.5 ppm
Nitrogen oxides	0.5 ppm

Table 5 Range and resolution of emission parameters

Gas measured	Measuring range	Resolution
CO	0 – 10% Vol	0.01%
CO <sub>2</sub>	0 – 20% Vol	0.1%
HC	0 – 15,000 ppm	1 ppm
O <sub>2</sub>	0 – 25% Vol	0.01%
NO <sub>x</sub>	0 – 10,000 ppm	1 ppm

### 3 Calculation

#### 3.1 Energy analysis

The compound energy of fuel is changed in to heat energy produced during combustion ( $Q_{in}$ ). The heat produced during combustion is utilized in different forms as brake power ( $Q_s$ ), energy lost by engine cooling water ( $Q_w$ ), energy conceded by emission of gases

( $Q_e$ ) and loss due to friction, radiation and energy spent to surroundings as unaccounted losses ( $Q_u$ ).

Heat energy due to combustion of fuel can be expressed as,

$$Q_{in} = [\dot{m}_f \times \text{LHV}], \text{ kW} \quad (1)$$

Shaft power available in the output shaft is calculated by,

$$Q_s = \text{BP} = \left[ \frac{2 \times \pi \times N \times W \times r}{60 \times 1000} \right], \text{ kW} \quad (2)$$

Thermal efficiency with respect to output shaft is given by,

$$\text{BTE} = \left[ \frac{\text{BP} \times 3600 \times 100}{Q_{in}} \right] \% \quad (3)$$

The rate of fuel consumed during combustion per unit power produced can be articulated as,

$$\text{BSEC} = \frac{[\dot{m}_f \times \text{LHV}] \left( \frac{\text{kJ}}{\text{s}} \right)}{\text{BP}}, \text{ kW} \quad (4)$$

Energy absorbed in engine cooling water in unit time is specified by,

$$Q_w = [\dot{m}_w \times C_{pw} \times (T_{ewo} - T_{ewi})], \text{ kW} \quad (5)$$

Energy lost through exhaust gases per unit time is found as,

$$Q_e = [(\dot{m}_a + \dot{m}_f) \times C_{pe} \times (T_{eci} - T_{amb})], \text{ kW} \quad (6)$$

The uncounted loss per unit time is

$$Q_u = [Q_{in} - (Q_s + Q_w + Q_e)], \text{ kW} \quad (7)$$

### 3.2 Exergy analysis

Availability is the determined convenient work that will be obtained through thermodynamic process. The conversion of fuel energy in to heat energy of a fuel is seemed as useful availability ( $A_s$ ), availability in cooling water ( $A_w$ ), exhaust gas availability ( $A_u$ ) and destructed availability ( $A_d$ ) due to friction, radiation and heat transfer to surrounding, etc. The availability expressions are determined from the law of exergy.

Availability in fuel input as,

$$A_{in} = \left[ \frac{1.0338 \times \dot{m}_f \times \text{LHV}}{3600} \right], \text{ kW} \quad (8)$$

$$A_s - \text{Shaft power or brake power, kW} \quad (9)$$

Cooling water availability in attained from,



$$A_w = \left[ Q_w - \{ \dot{m}_w \times C_{pw} \times T_{amb} \times \ln \left( \frac{T_{ewo}}{T_{ewi}} \right) \} \right], kW \tag{10}$$

Availability in exhaust gases is found as,

$$A_e = Q_e + \left[ (\dot{m}_a + \dot{m}_f) \times T_{amb} \times \left\{ C_{pe} \times \ln \left( \frac{T_{amb}}{T_{eci}} \right) - R_e \times \ln \left( \frac{P_{amb}}{P_e} \right) \right\} \right], kW \tag{11}$$

where  $R_e$  is emission gas constant in J/kg/K, calculated from,  $R_e = \text{Universal gas constant } (\bar{R}_u \text{ in kJ/kmol K}) / \text{molecular weight } (M \text{ in kg/kmol})$

Destructed availability is expressed as,

$$A_d = [A_{in} - (A_s + A_w + A_e)], kW \tag{12}$$

Exergy efficiency is given by,

$$\eta_{II} = \left[ 1 - \left( \frac{A_d}{A_{in}} \right) \right] \times 100\% \tag{13}$$

Entropy generation due to irreversibility is given as,

$$S = (A_d / T_{amb}), kW/K \tag{14}$$

### 3.3 Error analysis

The errors accompanied with engine performance and combustion parameters in VCR engine are considered in this section. The errors were found using minimum output value and accuracy of the instrument. This method is used to find uncertainties (Table 4) in the various experimental findings. The repeatability in error measurement was considered for error measurement (Murugapoopathi & Vasudevan, 2021). If R is the measured quantity of uncertainty,

$$\frac{\partial R}{R} = \left\{ (\partial x_1 / x_1) + (\partial x_2 / x_2) \dots + (\partial x_n / x_n) \right\}^2 \tag{15}$$

where,  $(\partial x_1 / x_1), (\partial x_2 / x_2)$  etc. are the errors in independent variables.

$\partial x_1$ -Measuring instrument accuracy,

$x_1$ -Minimum output measured.

## 4 Results and discussion

### 4.1 Energy analysis

The conversions of fuel energy into thermal energy per unit duration using various methods at various compression ratios, biodiesel ratios, and supercharging rates at 80% load are analyzed. Figure 2. depicts the energy changes with different fuel mixtures and data from five CRs are averaged and incorporated into the VCR engine to investigate the effect of supercharging. When the engine was switched from naturally aspirated (NAE)

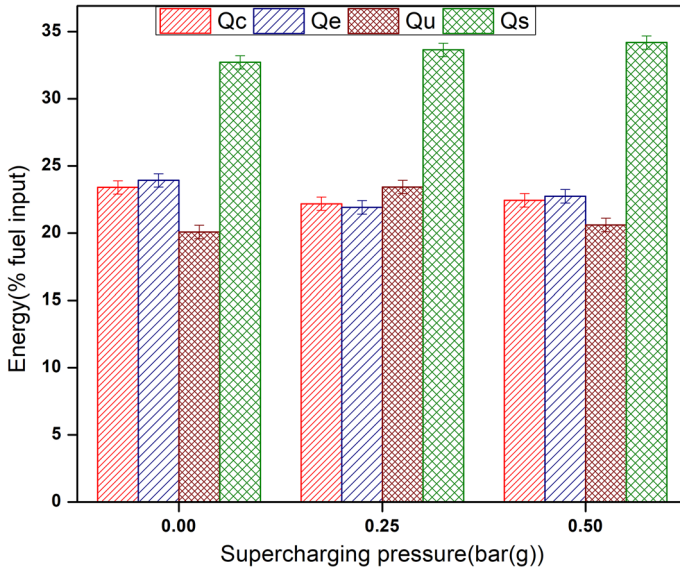


**Fig. 2** Variation in Energy (% fuel input) and supercharging pressures

to supercharged (SCE) under average conditions, the brake power and energy carried to exhaust gases increased by 1.67% and 6.87%, respectively. The amount of energy absorbed by cooling water is lowered by 4.97%, while the amount of energy lost due to friction and heat transfer is reduced by 3.93%. As shown in Fig. 3, the BTEs of diesel, B20, and B40 are 32.78%, 39.83%, and 33.53%, respectively, on an average CR of 20 at 1.25 bar pressure

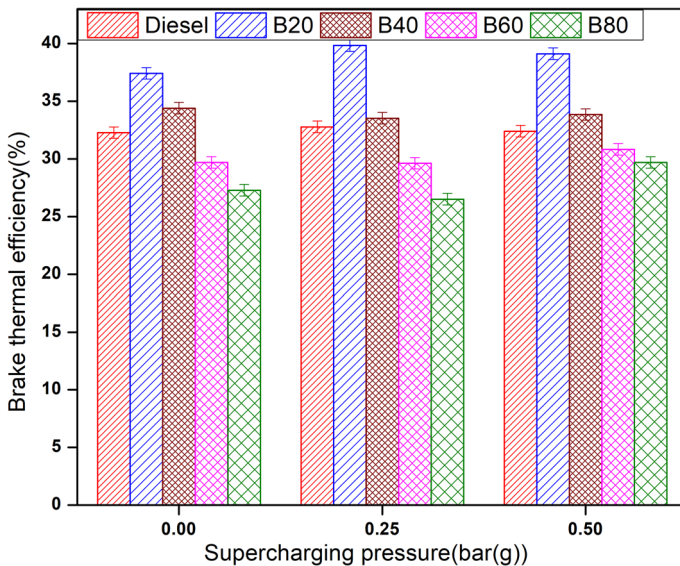


**Fig. 3** Variation in BTE and fuel blends

at the inlet pipe. Due to finer atomized biodiesel particles and low viscosity at a higher airflow rate and a higher CR, the BTE of B20 improved in comparison with B40 and diesel Leo et al. (2021).

This affords adequate time for mixing and evaporating fuel for biodiesel combustion. When compared to diesel, the BSEC and mass flow rate of B20 are lowered by 17.35% and 10.55%, respectively, on an average CR and airflow rate, as illustrated in the Figs. 4 and 5. The maximal BTE was raised by a micro-explosion of biodiesel at a higher airflow rate. In comparison with a naturally aspirated engine, the BSEC and mass flow rate of fuel at 0.25 bar (g) reduce by 1.36% and 2.54%, respectively, at the identical settings. On an average fuel blend, the maximum combustion pressure of a supercharged engine improves by 5.1%, while the HRR reduces by 3.1%, as shown in Fig. 6. At the same time, supercharging improves the combustion of fuel blends while reducing the rate of heat emission in the cylinder Thodda et al. (2020).

On average, there is a drop in EGT of 3.73% on the change from NAE to SCE, as depicted in Fig. 7. There was a rise in BTE, Pmax, and shaft power and a fall in BSEC, HRR, fuel flow rate, and EGT in an averaged CR, with a supercharged engine, compared to a naturally aspirated engine. The variations in supercharging pressure are presented in Fig. 8. With the advancement of fuel mode, the energy transferred to cooling water and shaft energy of fuel blends rises by 21.28% and 6.62% compared to diesel, respectively. Heat energy diffused into exhaust gas and unaccounted losses are reduced by 1.05% and 24.62%, respectively, for similar settings. At B20, the BTEs are obtained as 37.42%, 39.83%, and 39.12% for 1 atm, 1.25 and 1.5 bar pressure, respectively, in comparison with 32.27%, 32.78%, and 32.4% diesel, respectively.

With the fuel mode advanced to B40, the BTEs for 1, 1.25, and 1.5 pressures obtained in the input pipe are determined to be 34.4%, 33.53%, and 33.85%, respectively. The energy study revealed that supercharging in diesel and B20 improved BTEs, but that the

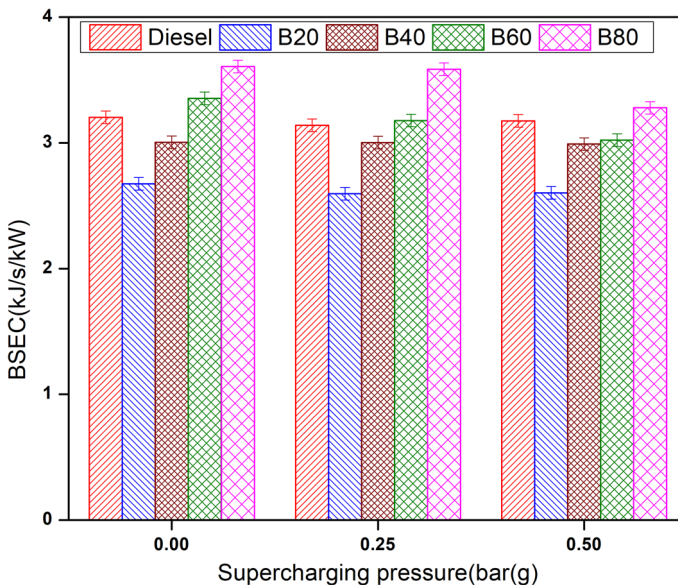


Fig. 4 Variation in BSEC and supercharging pressures

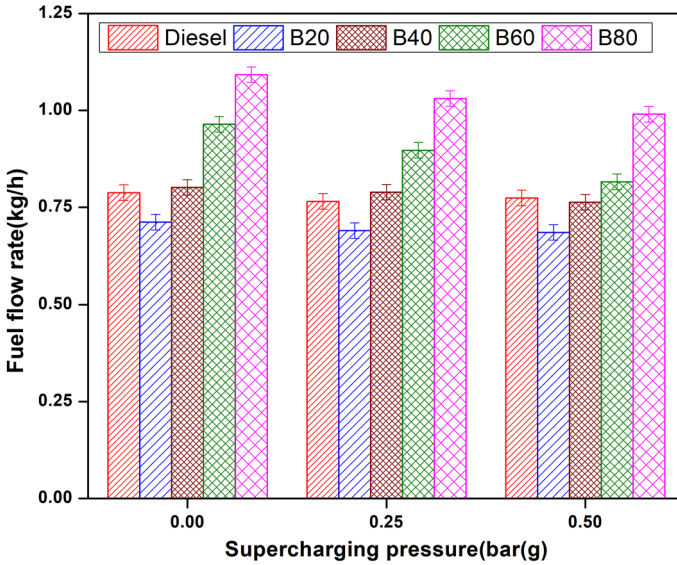


Fig. 5 Variation in Fuel flow rates and supercharging pressures

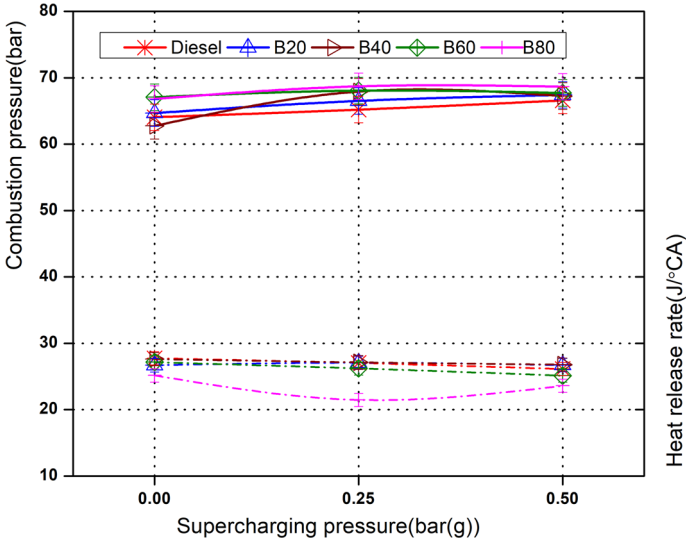


Fig. 6 Variation in Combustion pressure with HRR and supercharging pressures

increase in biodiesel blend % increased viscosity even more (Santhosh & Padmanabhan 2016b). Following that, thanks to the expansion of biodiesel blends, BTEs decrease. For diesel, B20, and B40,  $P_{max}$  increases by 4.03%, 4.24%, and 6.9%, respectively. For similar operating conditions, HRR for diesel and B40 drops to 5.8% and 3.91%, respectively (Sarikoc et al. 2020).

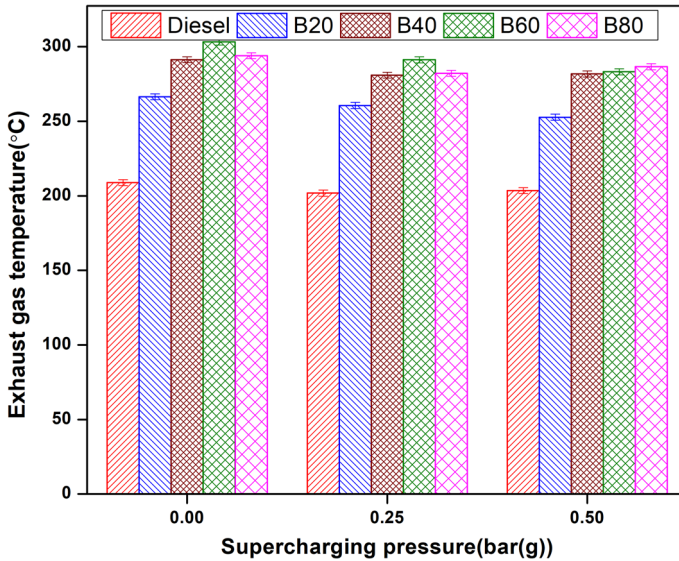


Fig. 7 Variation in Exhaust gas temperature and supercharging pressures

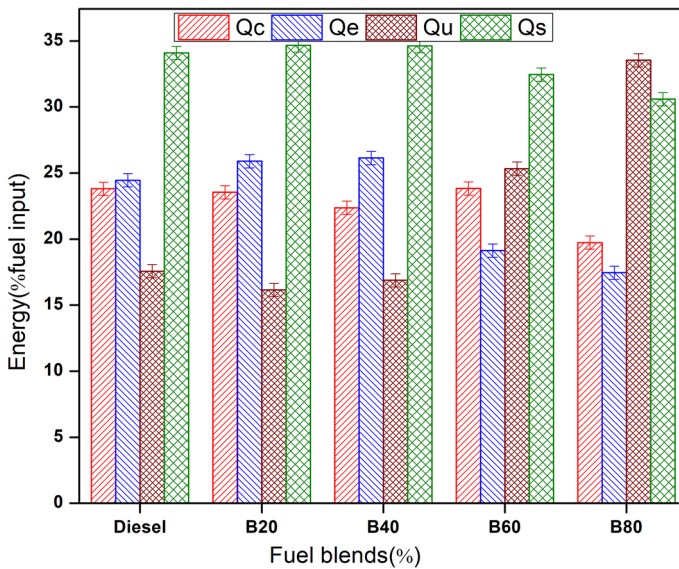


Fig. 8 Variation in Energy (% fuel input) and fuel blends

With the advancement of supercharging, BTE, Pmax, and shaft energy were improved, whereas BSEC, the mass flow rate of fuel, HRR, and EGT were decreased. The findings revealed that finer fuel droplets, a different fuel spray pattern, and a larger energy content of lower biodiesel blends, as well as averaged CR with airflow variation, considerably

improve the thermal efficiency, shaft energy, and maximum pressure. Due to its high thermal efficiency, the lower volatility nature of biodiesel, CR, and supercharging, there was a decline in BSEC, fuel flow rate, HRR, and EGT at the same time (Thulasiram et al., 2021).

## 4.2 Exergy analysis

The availability of energy at various techniques in the unit interval at various combinations of fuel blends and supercharging pressure with an 80% load is considered in Fig. 9. The effect of various energy variations on supercharging pressure in biodiesel and diesel mixtures is averaged. With the increase in supercharging pressure from normal atmospheric pressure to 1.5 bar, brake power and exhaust gas availability increased by 1.52% and 5.12%, respectively.

At the same conditions, the availability of cooling water and destroyed water drops by 17.2% and 3.78%, respectively. The data of five CRs is averaged and presented in Fig. 10 to explore the effect of fuel blends on exergy changes under supercharging. Switching from diesel to B40 fuel increases shaft and water availability by 6.61% and 33.1%, respectively. The exhaust gas availability and the destroyed availability are found to be 0.3% and 4.43%, respectively, under identical conditions.

Figures 11 and 12 show the energy efficiency and irreversibility loss as supercharging pressure varies with averaged compression ratio and fuel mixtures. According to exergy study, the maximum released energy of 66.57% is converted into useful work output. As supercharging, pressures vary, energy efficiency increases by 2.66% while entropy generation decreases by 1.7%. By switching from diesel to B40, the exergy efficiency increases by 3.45%, and the entropy output decreases by 13.8%. Because of their superior atomization and higher energy content at appropriate airflow, biodiesel B20 and B40 blends boost the

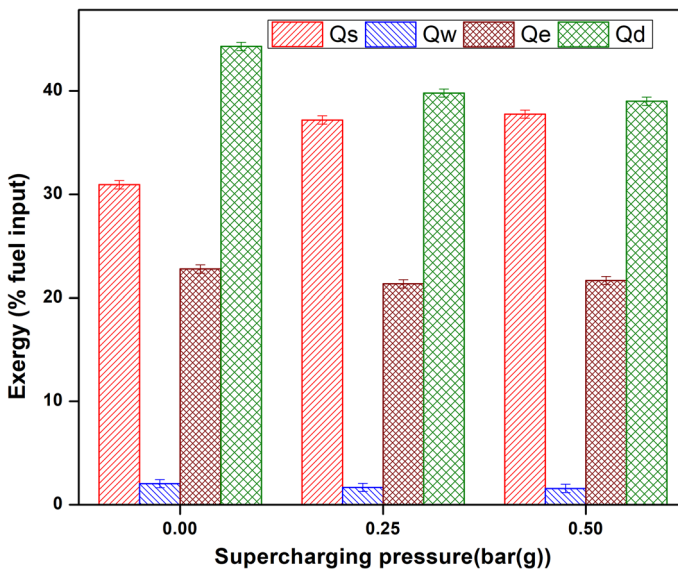


Fig. 9 Variation in Exergy (% fuel input) and supercharging pressures

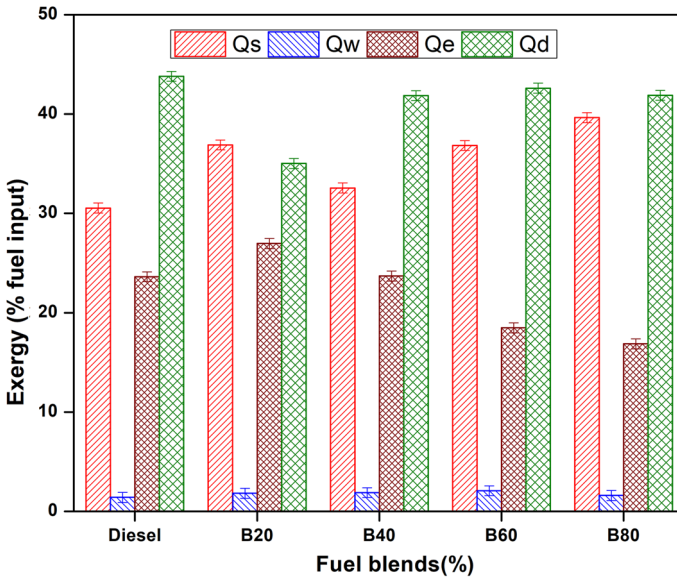


Fig. 10 Variation in Energy (% fuel input) and fuel blends

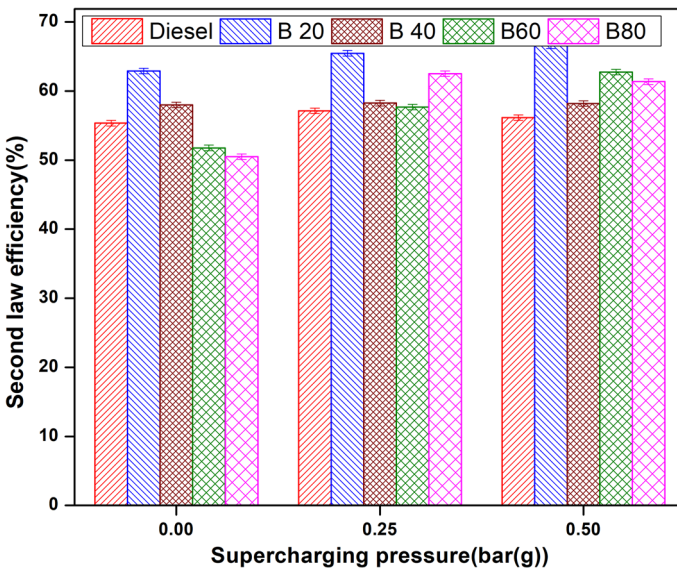


Fig. 11 Variation in Exergy efficiency and supercharging pressures

exergy efficiency. For the same settings as diesel and higher blends, the better combustion efficiency of biodiesel blends experienced a decline in entropy generation (Rakopoulos & Giakoumis 2006).

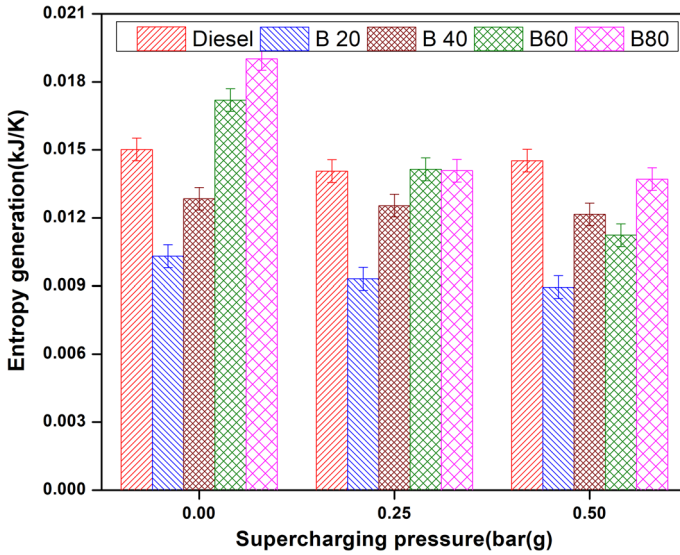


Fig. 12 Variation in Entropy generation and supercharging pressures

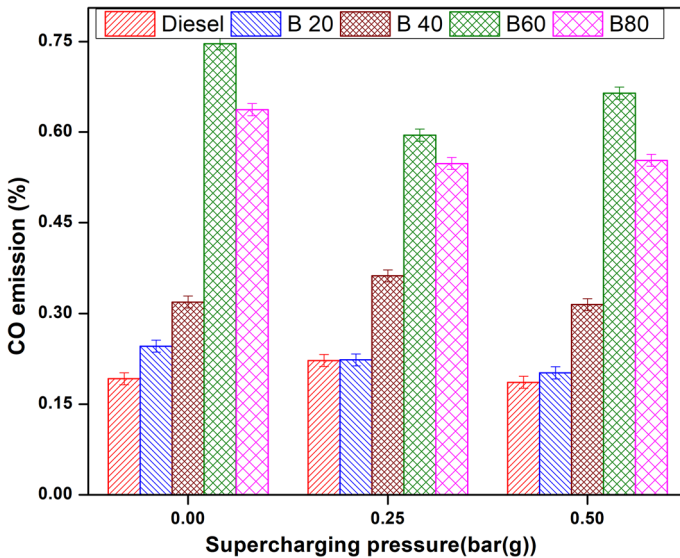


Fig. 13 Variation in CO emission and supercharging pressures

### 4.3 Emission analysis

The effect of fuel blends on the average compression ratio with variable supercharging pressure has been discussed. To evaluate the effect of supercharging, the fuel mixture and CR were averaged and included in Figs. 13, 14, 15 and 16. CO, HC, and NO<sub>x</sub> emissions fall by 7.51%, 6.08%, and 5.42%, respectively, when supercharging pressure is increased



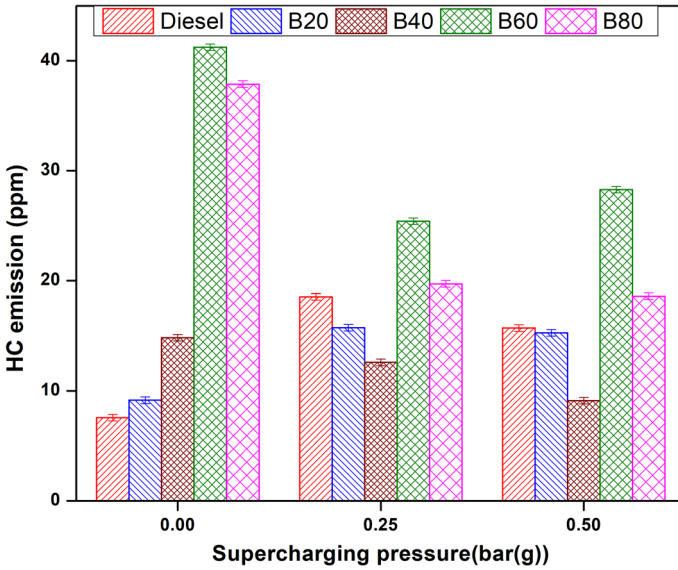


Fig. 14 Variation in HC emission and supercharging pressures

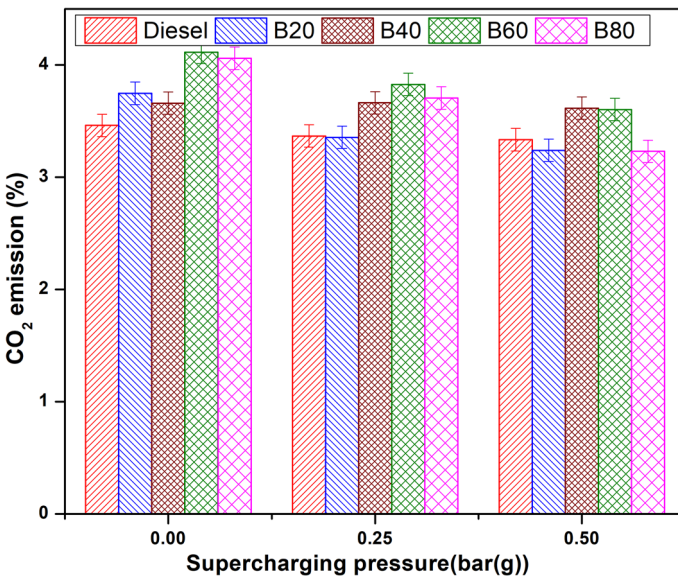


Fig. 15 Variation in CO<sub>2</sub> emission and supercharging pressures

from 1 atm. to 1.5 bar. This is due to the increased airflow rate, which improves combustion when the CR is at its best. The rise in in-cylinder temperature associated with high CR and maximum load operation causes an increase in NO<sub>x</sub> emissions. The effect of supercharging and averaging CR lowers the in-cylinder temperature. Insufficient airflow,

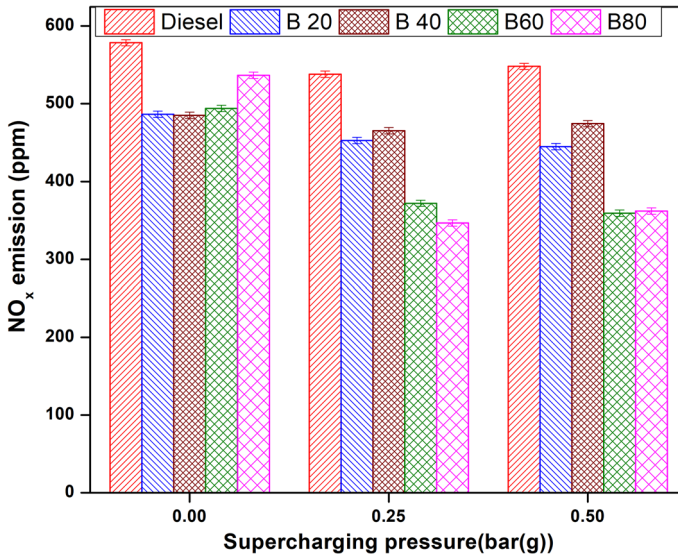


Fig. 16 Variation in NO<sub>x</sub> emission and supercharging pressures

inadequate atomization, and the position of the fuel injector are the main causes of CO and HC emissions.

This can be overcome by providing enough air, and a change in CR minimizes the CO and HC gaseous particles released. Changing the fuel mode from diesel to B40 reduced CO and CO<sub>2</sub> emissions by 39.76% and 3.65%, respectively, on an average SC pressure. Because of the reduction in in-cylinder temperature and evaporation of fuel droplets with coupled CR and supercharging, the HC and NO<sub>x</sub> gases are reduced by 16.67% and 14.41%, respectively, for equivalent operations (Şanlı & Uludamar, 2020). The effect of supercharging and the development of CR reduce CO emissions greatly, but the poor quality of fuel and lower energy content at higher CR increase CO and HC emissions of higher mixes in NAE dramatically (Bora & Saha, 2016). However, when compared to other emissions, NO<sub>x</sub> emissions are significantly reduced by lowering the in-cylinder temperature and modifying the airflow fluctuations (Santhosh & Padmanaban, 2016a).

## 5 Conclusions

By observation, energy and emission investigation of blends of biodiesel working at various CRs and supercharging pressure were examined through water cooled, VCR engine. The biodiesel used in this work is methyl esters of rubber oil produced from rubber seeds, blended with diesel on volume basis. The experiment was carried out at 80% load for 9 combinations of operating parameters consists of five fuel blends, viz. diesel, B20 and B40 and three SC gauge pressures, viz. 0, 0.25 and 0.5 bar under averaged CRs. The energy analysis reveals that the impact of SC pressure of 0.25 bar gauge pressure under averaged CR 20 with averaged fuel combinations diesel, B20 and B40 results in a decrease of both uncounted losses and cooling water losses in comprehend with B60, B80 and diesel.

- Supercharging reduces cooling water loss by 4.11% while slightly increasing unaccountable losses by 2.64% for average fuel blends and compression ratios.
- For the same operating conditions, shaft energy improves by 4.31% but exhaust gas energy flow reduces by 5.18%.
- Supercharging resulted in a 2.99% increase in BTE and a 7.54% decrease in BSEC.
- Peak pressure increases by 3.75% with supercharging, whereas the heat release rate lowers by 4.46% under the same operating conditions.
- The irreversibility and cooling water availability were reduced by 11.97% and 22.51%, respectively, with supercharging.
- CO and HC emissions were lowered by 10.26% and 21.41%, respectively, when diesel was compared to supercharging.
- The NO<sub>x</sub> emission was decreased by 15.14% but CO<sub>2</sub> emission was increased by 10.59% with supercharging.
- For averaged fuel blends and compression ratios, supercharging increased second law efficiency by 9.51%.
- On average, at 1.25 bar pressure, there was a significant increase in BTE of 39.83% for CR 20. With the use of supercharging and CR, energy is transmitted to the shaft, and exhaust energy flow increases.
- On average, the exergy analysis indicates that 33.5% of the fuel energy is recoverable from available energy, and the work output availability surges up to 36.9% of 1.25 bar pressure under the averaged CR of B20.

The outcomes exposed that the result of supercharging, for utilization of fuel energy of bio-fuel, was articulated as a suitable one in comparison with diesel fuel. From a thermodynamic point of view, the lower blends of rubber seed oil B20 and B40 under average CR 20 at a combination of 1.25 bar supercharging pressure should be implemented to meet the stringent emission norms in the VCR engine without any modifications.

## Declarations

**Conflict of interest** On behalf of author, the corresponding author states that there is no conflict of interest.

## References

- Bora, B. J., & Saha, U. K. (2016). Estimating the theoretical performance limits of a biogas powered dual fuel diesel engine using emulsified rice bran biodiesel as pilot fuel. *Journal of Energy Resources Technology*, 138(2), 021801. <https://doi.org/10.1115/1.4031836>
- Chaudhary, V., & Gakkhar, R. P. (2021). Exergy analysis of small DI diesel engine fueled with waste cooking oil biodiesel. *Energy Sources, Part a: Recovery, Utilization, and Environmental Effects*, 43(2), 201–215. <https://doi.org/10.1080/15567036.2019.1624875>
- Debnath, B. K., Saha, U. K., & Sahoo, N. (2013). Theoretical route toward the estimation of second law potential of an emulsified palm biodiesel run diesel engine. *Journal of Energy Engineering*, 140(3), A4014007. [https://doi.org/10.1061/\(ASCE\)EY.1943-7897.0000134](https://doi.org/10.1061/(ASCE)EY.1943-7897.0000134)
- Duarte-Forero, J., Mendoza-Casseres, D., & Valencia-Ochoa, G. (2021). Energy, Exergy, and Emissions (3E) assessment of a low-displacement engine powered by biodiesel blends of palm oil mill effluent (POME) and hydroxy gas. *Thermal Science and Engineering Progress*. <https://doi.org/10.1016/j.tsep.2021.101126>
- Gnanamani, S., Gaikwad, P. U., Subramaniam, L., & Chandralingam, R. (2021). Exergy analysis in diesel engine with binary blends. *Thermal Science*, 00, 273–273. <https://doi.org/10.2298/TSCI200808273G>

- Leo, G. L., Thodda, G., & Murugapoopathi, S. (2021). Experimental investigation on effects of gasoline premixed-Al<sub>2</sub>O<sub>3</sub> additive blended fish oil biodiesel fuelled HCCI-DI engine. In *Journal of Physics: Conference Series*. (Vol. 2054, No. 1, p. 012040) IOP Publishing. <https://doi.org/10.1088/1742-6596/2054/1/012040>
- Mahabadipour, H., Srinivasan, K. K., & Krishnan, S. R. (2019). An exergy analysis methodology for internal combustion engines using a multi-zone simulation of dual fuel low temperature combustion. *Applied Energy*, 256, 113952. <https://doi.org/10.1016/j.apenergy.2019.113952>
- Murugapoopathi, S., & Vasudevan, D. (2019a). Energy and exergy analysis on variable compression ratio multi-fuel engine. *Journal of Thermal Analysis and Calorimetry*, 136(1), 255–266. <https://doi.org/10.1007/s10973-018-7761-2>
- Murugapoopathi, S., & Vasudevan, D. (2019b). Performance, combustion and emission characteristics on VCR multi-fuel engine running on methyl esters of rubber seed oil. *Journal of Thermal Analysis and Calorimetry*, 138(2), 1329–1343. <https://doi.org/10.1007/s10973-019-08281-x>
- Murugapoopathi, S., & Vasudevan, D. (2021). Experimental and numerical findings on VCR engine performance analysis on high FFA RSO biodiesel as fuel using RSM approach. *Heat and Mass Transfer*, 57(3), 495–513. <https://doi.org/10.1007/s00231-020-02961-3>
- Odibi, C., Babaie, M., Zare, A., Nabi, M. N., Bodisco, T. A., & Brown, R. J. (2019). Exergy analysis of a diesel engine with waste cooking biodiesel and triacetin. *Energy Conversion and Management*, 198, 111912. <https://doi.org/10.1016/j.enconman.2019.111912>
- Rakopoulos, C. D., & Giakoumis, E. G. (2006). Second-law analyses applied to internal combustion engines operation. *Progress in Energy and Combustion Science*, 32(1), 2–47. <https://doi.org/10.1016/j.pecs.2005.10.001>
- Şanlı, B. G., & Uludamar, E. (2020). Energy and exergy analysis of a diesel engine fuelled with diesel and biodiesel fuels at various engine speeds. *Energy Sources, Part a: Recovery, Utilization, and Environmental Effects*, 42(11), 1299–1313. <https://doi.org/10.1080/15567036.2019.1635229>
- Santhosh, M., & Padmanaban, K. P. (2016a). Experimental investigation on engine performances, combustion characteristics and emission of exhaust gases of VCR engine fuelled with cottonseed oil methyl ester blended with diesel. *International Journal of Green Energy*, 13(14), 1534–1545. <https://doi.org/10.1080/15435075.2014.977438>
- Santhosh, M., & Padmanaban, K. P. (2016b). Experimental studies on variable compression ratio engine fuelled with cottonseed oil methyl ester biodiesel. *International Journal of Oil, Gas and Coal Technology*, 12(1), 81–104. <https://doi.org/10.1504/IJOGCT.2016b.075842>
- Sarıkoç, S., Örs, İ., & Ünalın, S. (2020). An experimental study on energy-exergy analysis and sustainability index in a diesel engine with direct injection diesel-biodiesel-butanol fuel blends. *Fuel*, 268, 117321. <https://doi.org/10.1016/j.fuel.2020.117321>
- Thodda, G., Madhavan, V. R., & Thangavelu, L. (2020). Predictive modelling and optimization of performance and emissions of acetylene fuelled CI engine using ANN and RSM. *Energy Sources, Part a: Recovery, Utilization, and Environmental Effects*. <https://doi.org/10.1080/15567036.2020.1829191>
- Thulasiram, R., Murugan, S., Ramasamy, D., & Sundaramoorthy, S. (2021). Modelling and evaluation of combustion emission characteristics of COME biodiesel using RSM and ANN—a lead for pollution reduction. *Environmental Science and Pollution Research*. <https://doi.org/10.1007/s11356-021-12757-5>

**Publisher's Note** Springer Nature remains neutral with regard to jurisdictional claims in published maps and institutional affiliations.

Springer Nature or its licensor holds exclusive rights to this article under a publishing agreement with the author(s) or other rightsholder(s); author self-archiving of the accepted manuscript version of this article is solely governed by the terms of such publishing agreement and applicable law.